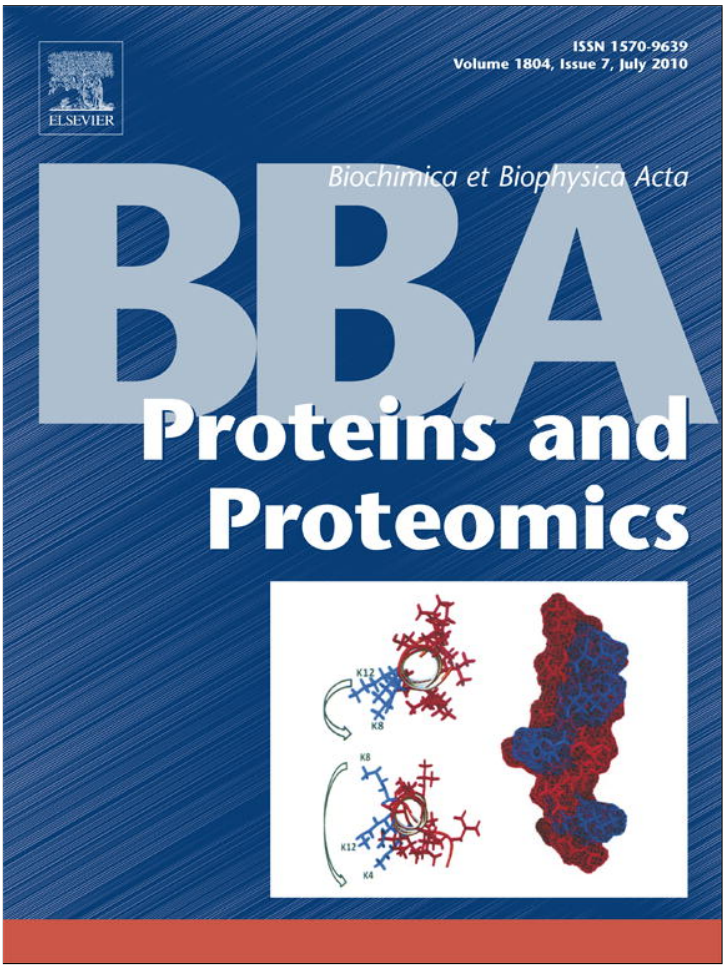

Biochimica et Biophysica Acta 1804 (2010) 1542–1547

Contents lists available at ScienceDirect

Biochimica et Biophysica Acta

journal homepage: www.elsevier.com/locate/bbapap

Structural basis for the different activities of yeast Grx1 and Grx2

Wei-Fang Li [1], Jiang Yu [1], Xiao-Xiao Ma, Yan-Bin Teng, Ming Luo, Ya-Jun Tang, Cong-Zhao Zhou *

Hefei National Laboratory for Physical Sciences at Microscale and School of Life Sciences, University of Science and Technology of China, Hefei Anhui 230027, PR China

ARTICLE INFO

Article history:
Received 28 January 2010
Received in revised form 24 March 2010
Accepted 13 April 2010
Available online 24 April 2010

Keywords:
Glutaredoxin
Glutathione
Crystal structure
Redox state
Conformational rearrangement
Glutathione-disulfide reductase activity

ABSTRACT

Yeast glutaredoxins Grx1 and Grx2 catalyze the reduction of both inter- and intra-molecular disulfide bonds using glutathione (GSH) as the electron donor. Although sharing the same dithiolic CPYC active site and a sequence identity of 64%, they have been proved to play different roles during oxidative stress and to possess different glutathione-disulfide reductase activities. To address the structural basis of these differences, we solved the crystal structures of Grx2 in oxidized and reduced forms, at 2.10 Å and 1.50 Å, respectively. With the Grx1 structures we previously reported, comparative structural analyses revealed that Grx1 and Grx2 share a similar GSH binding site, except for a single residue substitution from Asp89 in Grx1 to Ser123 in Grx2. Site-directed mutagenesis in combination with activity assays further proved this single residue variation is critical for the different activities of yeast Grx1 and Grx2.

1. Introduction

All aerobic organisms are exposed to reactive oxygen species (ROS), such as H_2O_2, the superoxide anion (O_2^-) and the hydroxyl radical (OH^-), during the course of normal aerobic metabolism or after exposure to radical-generating compounds [1]. Accumulation of ROS can cause oxidative damage to various biological molecules, including proteins, nucleic acids, cell membranes and lipids, which is associated with various diseases processes such as cancer, aging and neurodegenerative disorders [2,3]. In all organisms, the glutaredoxins/glutathione (Grxs/GSH) and thioredoxin (Trx) systems are the most important to maintain the cellular redox homeostasis [4–7].

Grxs are a group of GSH-dependent thiol-disulfide oxidoreductases [8–13], involved in a series of essential biosynthetic reactions and regulation of many biological processes, especially in the defense of oxidative stress. Grxs prefer catalyzing the GSH-mixed disulfide bonds [14,15], indicating their roles in glutathionylation and deglutathionylation of proteins in cellular response to oxidative stress [16,17]. To date, eight yeast Grxs have been described in the chronological order by identification date [18] and classified into two subfamilies based on the active site motif. Grx1/YCL035C and Grx2/YDR513W are dithiol cytosolic Grxs, which contain a conserved CPYC motif at the active site. Despite the high degree of homology between Grx1 and Grx2 (64% identity), evidence has shown that they play distinct roles in normal growth and stress conditions. The *GRX1* mutant is sensitive to oxidative stress induced by the superoxide anion, whereas a strain that lacks *GRX2* gene is sensitive to hydrogen peroxide [19]. Grx8/YLR364W, a third putative cytosolic dithiol Grx of 109 residues, was identified in silico recently [18]. The deletion of Grx8 does not result in a decrease of growth rate under oxidative stress conditions nor does it enhance the defects of *GRX1* and *GRX2* single or double deletions [18]. Grx3/YDR098C, Grx4/YER174C, Grx5/YPL059W, Grx6/YDL010W and Grx7/YBR014C are monothiol Grxs with an active site motif of CXXS [20–22]. Grx3 and Grx4 are required for the regulation of the iron-dependent transcriptional factor Aft1 in the nuclei [23], whereas Grx5 involves in the synthesis or assembly of iron–sulfur (Fe–S) clusters in the mitochondrial matrix [22,24], all of which have an active site of CGFS. The active site of Grx6 and Grx7 are CSYS and CPYS, respectively, which are responsible for the regulation of the sulfhydryl redox state at the oxidative conditions of the early secretory pathway vesicles [21].

Grx1 exists in both cytoplasm and nucleus. Upon the redox transition, residues around the active site would undergo conformational changes to reinforce the GSH binding [25]. Grx2 is expressed in two isoforms via alternative translation with different start codons, with the shorter isoform (11.9 kDa) retained in the cytosol while the longer one (15.9 kDa) translocated to the mitochondrial matrix where it is either processed by the mitochondrial processing peptidase to a short soluble isoform that localizes to the matrix or left unprocessed and retained in the outer mitochondrial membrane [26,27]. In addition to the different subcellular localizations, the binding affinity

Abbreviations: Grx, glutaredoxin; ROS, reactive oxygen species; GSH, reduced glutathione; GR, glutathione reductase; HED, β-hydroxyethyl disulfide; GSSG, oxidized glutathione, glutathione disulfide; β-ME-SG, glutathionylated β-mercaptoethanol; HEDS assay, glutathione:bis-(2-hydroxyethyl)-disulfide transhydrogenase assay

* Corresponding author. Tel./fax: +86 551 3600406.
E-mail address: zcz@ustc.edu.cn (C.-Z. Zhou).

[1] Both authors contributed equally to this work.

1570-9639/$ – see front matter © 2010 Elsevier B.V. All rights reserved.
doi:10.1016/j.bbapap.2010.04.010

towards GSH is also supposed to contribute to their physiological divergences.

We solved the crystal structures of Grx2 in oxidized and reduced forms, and revealed the redox-induced conformational rearrangements in the active site region. Structural comparisons between the reduced Grx2 and glutathionylated Grx1 which we had solved previously [25] indicated that a single residue change from Asp89 in Grx1 to Ser123 in Grx2, which might lead to their difference in glutathione-disulfide reductase activities (*EC 1.8.1.7*). To further verify this hypothesis, two mutants, Grx1D89S and Grx2S123D were constructed, and their glutathione-disulfide reductase activities were detected by the glutathione:bis-(2-hydroxyethyl)-disulfide transhydrogenase assay (HEDS assay). The comparative activity assays proved that the Asp89 in Grx1 or Ser123 in Grx2 is the key residue to the different activities of these two glutaredoxins.

2. Materials and methods

2.1. Cloning, expression and purification of Grx2, Grx1D89S and Grx2S123D in Escherichia coli

The yeast *GRX2* gene encoding the shorter isoform comprising residues from Met35 to Gln143 (without the signal peptide) was amplified by PCR with *S. cerevisiae* S288C genomic DNA as the template, and cloned into the vector pET15b (Novagen). Extra sequence encoding MGSSHHHHHHSSGLVPRGSH at N-terminal was added. The recombinant protein was expressed in BL21 (DE3) strain of *E. coli*, induced with 0.2 mM IPTG at 37 °C for 5 h when OD_{600nm} reached 0.6. Cells were collected by centrifugation and resuspended in the binding buffer (200 mM NaCl, 20 mM Tris–HCl, pH 7.0). After 3 min of sonication and centrifugation, the supernatant containing the soluble target protein was collected and loaded to a Ni–NTA column (GE Healthcare) equilibrated with binding buffer. The target protein was eluted with 300 mM imidazole, and loaded to a Superdex 75 16/60 column, equilibrated with the binding buffer. Fractions containing the recombinant Grx2 were pooled, desalted and concentrated to 10 mg/ml in a final buffer of 20 mM NaCl, 20 mM Tris–HCl, pH 7.0, and then applied to crystallization. Protein concentration was calculated by UV absorbance at 280 nm with an extinction coefficient of 4595 M^{-1} cm^{-1} (http://www.expasy.org/tools/protparam.html).

The Grx1D89S and Grx2S123D mutants were prepared with the QuickChange Site-Directed Mutagenesis Kit according to the manufacturer's recommendations (Stratagene). The pET28/*GRX1* [25] and pET15b/*GRX2* plasmids were used as templates with the primers containing the desired mutation (underlined): 5′-GGA GGC AAC AGC GAC TTG CAG GAA T-3′ (forward Grx1D89S), 5′-TG CAA GTC GCT GTT GCC TCC AAT AT-3′ (reverse Grx1D89S), 5′-GGT GGT AAC GAC GAT TTG GAA ACT T-3′ (forward Grx2S123D), 5′-TC CAA ATC GTC GTT ACC ACC AAT GT-3′ (forward Grx2S123D). The gene sequences were confirmed by automated DNA sequencing. Grx1D89S and Grx2S123D plasmids were used to transform Rossetta and BL21 (DE3) strain of *E. coli*, respectively. The expression and purification of Grx1D89S and Grx2S123D were similar as the Grx2 (above mentioned). Fractions containing the recombinant Grx1D89S, Grx2S123D, and Grx1, Grx2 were all pooled, desalted and concentrated to 50 μM in the buffer of 20 mM NaCl, 20 mM Tris–HCl, pH 8.5, 50% glycerol. Protein purity was checked by SDS-PAGE.

2.2. Crystallization, X-ray data collection, structure solution and refinement of Grx2 in different redox states

Crystals were grown at 16 °C in a hanging drop of 1.0 μl protein sample at 10 mg/ml in 20 mM NaCl, 20 mM Tris–HCl, pH 7.0 with equal volume of reservoir solution. Two forms of crystals were obtained in the condition of 30% PEG 4000, 0.2 M NH_4Ac and 0.1 M NaAc, pH 4.6. Octahedral crystals of the reduced Grx2 appeared in one day, whereas rod-shaped crystals of the oxidized Grx2 were found in one week.

The crystals were transferred to the cryoprotectant of the reservoir solution supplemented with 25% glycerol and flash cooled with liquid nitrogen. The X-ray diffraction data were collected at 100 K in a liquid nitrogen stream using a Rigaku MM007 X-ray generator (λ = 1.5418 Å) with a MarResearch 345 image-plate detector at School of Life Sciences, University of Science and Technology of China (USTC, Hefei, PR China). The data were processed by AUTOMAR 1.4 [28]. The Grx2 structures were solved by the molecular replacement method with the program CNS [29] using the atomic coordinates of oxidized yeast Grx1 as the search model (PDB code 3C1R). Structures were fitted and rebuilt with program O [30] and refined with REFMAC5 [31] and CNS [29]. The overall assessments of model quality were performed using PROCHECK [32]. The atomic coordinates of oxidized and reduced Grx2 have been deposited in the Protein Data Bank (http://www.rcsb.org/pdb) under the entries of 3CTF and 3CTG, respectively. Statistics of both structures are summarized in Table 1. All figures were prepared with PyMOL [33].

2.3. Assay for glutathione-disulfide reductase activity of Grxs

Glutathione-disulfide reductase activity was measured by the reduction of the mixed disulfide formed between HEDS and GSH [34]. Specific activities and substrate specificity towards glutathionylated substrates of yeast enzymes (Grx1, Grx2 and of each mutants

Table 1
Data collection and refinement statistics.

Data set	Oxidized Grx2	Reduced Grx2
PDB code	3CTF	3CTG
Space group	$P4_12_12$	$P4_3$
Unit cell (Å)	$a=48.770$, $b=48.770$, $c=96.446$, $\alpha=\beta=\gamma=90°$	$a=41.630$, $b=41.630$, $c=78.390$, $\alpha=\beta=\gamma=90°$
Resolution (Å)	28.05–2.10 (2.18–2.10)[a]	22.13–1.50 (1.55–1.50)
Observed reflections	45,508	14,685
Unique reflections	12,610	4694
R_{merge}[b] (%)	6.01 (27.36)	7.61 (14.11)
I/σ	7.1(2.3)	6.4 (3.3)
Average redundancy	3.56 (3.57)	2.91(2.97)
Completeness (%)	97.2 (95.3)	98.5 (99.4)
Mosaicity	0.125 +/− 0.032	0.290 +/− 0.073
R_{work}[c] (last shell)	22.1 (23.1)	19.6 (25.7)
R_{free}[d] (last shell)	24.6 (25.1)	20.0 (28.8)
Mean B factors (Å^2)	27.6	16.3
r.m.s.d. bond Length[e] (Å)	0.010	0.006
r.m.s.d. bond angles (°)	1.2	1.0
r.m.s.d. dihedral angles (°)	24.1	24.0
Ramachandran plot (residues, %)		
Most favored	96.8	97.9
Additionally allowed	3.2	2.1

[a] The values in parentheses refer to the highest resolution shell.

[b] $R_{merge} = \Sigma h \Sigma i |Iih - In| / \Sigma h \Sigma i Ih$, where Ih is the mean intensity of the i observations of reflection h.

[c] R-factor $= \Sigma h ||F_{obs}| - |F_{calc}|| / \Sigma |F_{obs}|$, where $|F_{obs}|$ and $|F_{calc}|$ are the observed and calculated structure factor amplitudes, respectively. Summation includes all reflections used in the refinement.

[d] R-free $= \Sigma ||F_{obs}| - |F_{calc}|| / \Sigma |F_{obs}|$, evaluated for a randomly chosen subset of 5% of the diffraction data not included in the refinement.

[e] Root mean square deviation from ideal values.

Grx1D89S, Grx2S123D) were monitored at 30 °C with a DU800 UV/visible spectrophotometer (Beckman Coulter). The reaction mixture, containing 100 mM Tris–HCl, pH 7.4, 0.25 mM NADPH, 0.5–2.5 mM GSH, 6 μg/ml yeast glutathione reductase (GR, Sigma-Aldrich), 0.07–2.5 mM HEDS and 40–200 nM Grx in a volume of 200 μl. GSH, GR, HEDS and NADPH were pre-incubated for 3 min for the formation of the mixed disulfide between GSH and HED. The assay was triggered by the addition of different Grxs to the optimum concentration. The decrease of absorbance at 340 nm was monitored to indicate the consumption of NADPH. Measured activities in all assays were corrected by subtracting the velocities of the control reactions without Grx. Three independent experiments were performed at each substrate concentrations and the apparent K_m and k_{cat} values were calculated by non-linear regression of Michaelis–Menten plots.

3. Results and discussions

3.1. Overall structure of Grx2

The overall structure of Grx2 is consistent with the glutaredoxin fold (Trx-like fold), with a core of four mixed β strands surrounded by five α helices. The central β sheet is composed of three antiparallel strands (β1, β3, β4) with strand β2 parallel to the adjacent β1 (Fig. 1A). Structural comparisons between Grx2 and glutathionylated Grx1 present the same secondary structure arrangement, characterized with one specifically GSH-shaped and highly positively charged binding groove, electronically complementary to the GSH molecule.

3.2. Redox-induced conformational rearrangements

Superposition of the main-chain atoms between the oxidized and reduced forms (residues from 36 to 143) of Grx2 gives an RMSD (root mean square deviation) of 0.3 Å, indicating a highly similar overall structure. Moreover, subsequent to the breakage of the disulfide between Cys61 and Cys64, the active site region from Thr59 to Lys65 undergoes similar conformational rearrangements (Fig. 1B), as previously observed in the structures of yeast Grx1 [25] and poxviral glutaredoxin [35]. Compared to the oxidized form, the orientation of carbonyl oxygen of Thr59 in the reduced form flips outwards to the solvent, with a 1.49 Å shift of its Cα atom. The solvent-exposed aromatic side chain of Tyr60 flips toward the GSH binding site with the hydroxyl group moving 10.91 Å, while the carbonyl oxygen of Tyr60 is reoriented to avoid steric hindrance. Furthermore the aromatic side chain of Tyr63 swivels toward the GSH binding site, resulting in its hydroxyl group to move 4.07 Å, which might make hydrophobic interactions with the γ-glutamyl moiety of GSH. In addition, the Nε atom of Lys65 forms polar interactions with carbonyl oxygen atoms of Thr59 and Cys61, at a distance of 2.40 and 3.10 Å, respectively. These polar interactions may contribute to the catalytic activity of Grx2, as indicated from assays of the corresponding residue Arg26 of pig glutaredoxin [36], which has only a marginal influence on p*K*a value of the N-terminal cysteine [37], and the mutation of which to Val remarkably decreased the enzymatic activity [38].

3.3. Residues crucial for GSH binding

In a previous work, we solved the crystal structure of glutathionylated yeast Grx1, in which GSH formed a disulfide bond with its N-terminal cysteine of the active site [25]. Sequence alignment of Grx1 and Grx2 demonstrates that residues involved in GSH binding are highly conserved, except for a single reside change of D89 in Grx1 to S123 in Grx2 (Fig. 2A). In detail, residues K24 and Q63 of Grx1 (K58 and Q97 of Grx2) are involved in interactions with the glycinyl moiety; residues TVP interact with the cysteinyl moiety; and residues NDD of Grx1 (NSD of Grx2) participate in fixing the γ-glutamyl moiety.

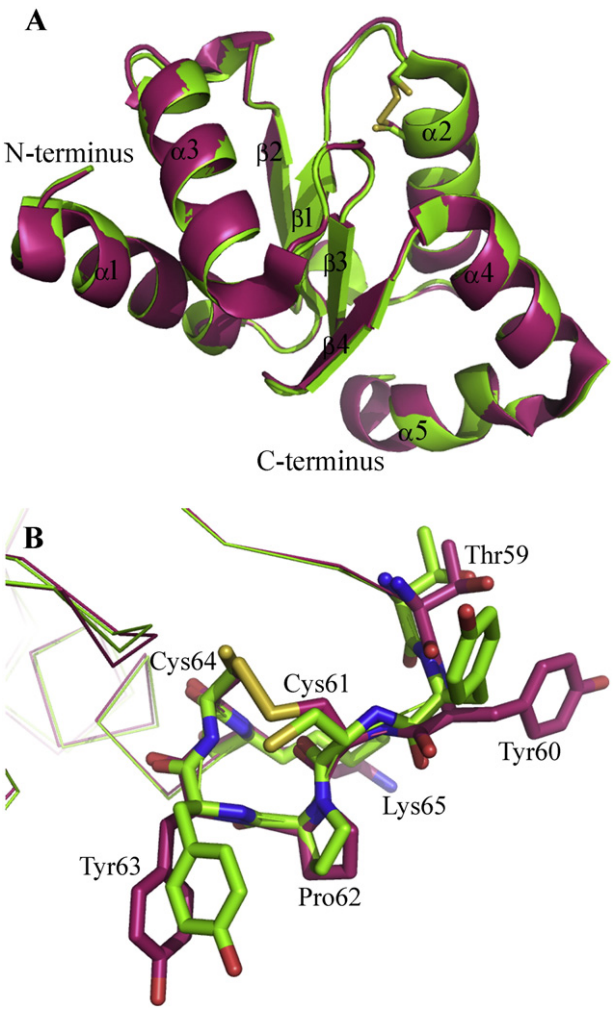

Fig. 1. Overall structure of Grx2 and conformational changes at the active site A) Cartoon representation of the superimposed overall structure of reduced (green) and oxidized (red) Grx2. Cysteines are represented as sticks. B) Redox-induced conformational rearrangements in the region from residues Thr59 to Lys65. Residues of the reduced and oxidized Grx2 are colored in green and red, respectively.

Besides their sequence similarities, superposition shows that Grx1 and Grx2 share a very similar overall structure with an RMSD of 0.642 Å (Fig. 2B). In glutathionylated Grx1, the side-chain carboxyl oxygen atoms of Asp89 form two hydrogen bonds with the γ-glutamyl moiety of GSH (Fig. 2C). In contrast, as shown in the structure solved by Discola et al. [39], the side-chain hydroxyl oxygen of Ser123 in Grx2 also forms two hydrogen bonds with the amide nitrogen and the carboxyl oxygen of γ-glutamyl moiety (Fig. 2D). However, the unequal hydrogen bond lengths and different van de Waals forces lead us to suppose that this single residue change from Asp to Ser critically affects the interaction at the binding vicinity of γ-glutamyl moiety, thereby differs the substrate binding affinity and/or glutathione-disulfide reductase activity of Grx1 and Grx2.

3.4. Difference of glutathione-disulfide reductase activity between Grx1 and Grx2

Grxs are originally assigned for their abilities to reduce the mixed disulfide of the glutathionylated β-mercaptoethanol (β-ME-SG) [34]. As the classic dithiol Grxs, both Grx1 and Grx2 could reduce the mixed disulfide with the electron donor GSH, which is in turn reduced by NADPH and glutathione reductase [40]. Using an optimum

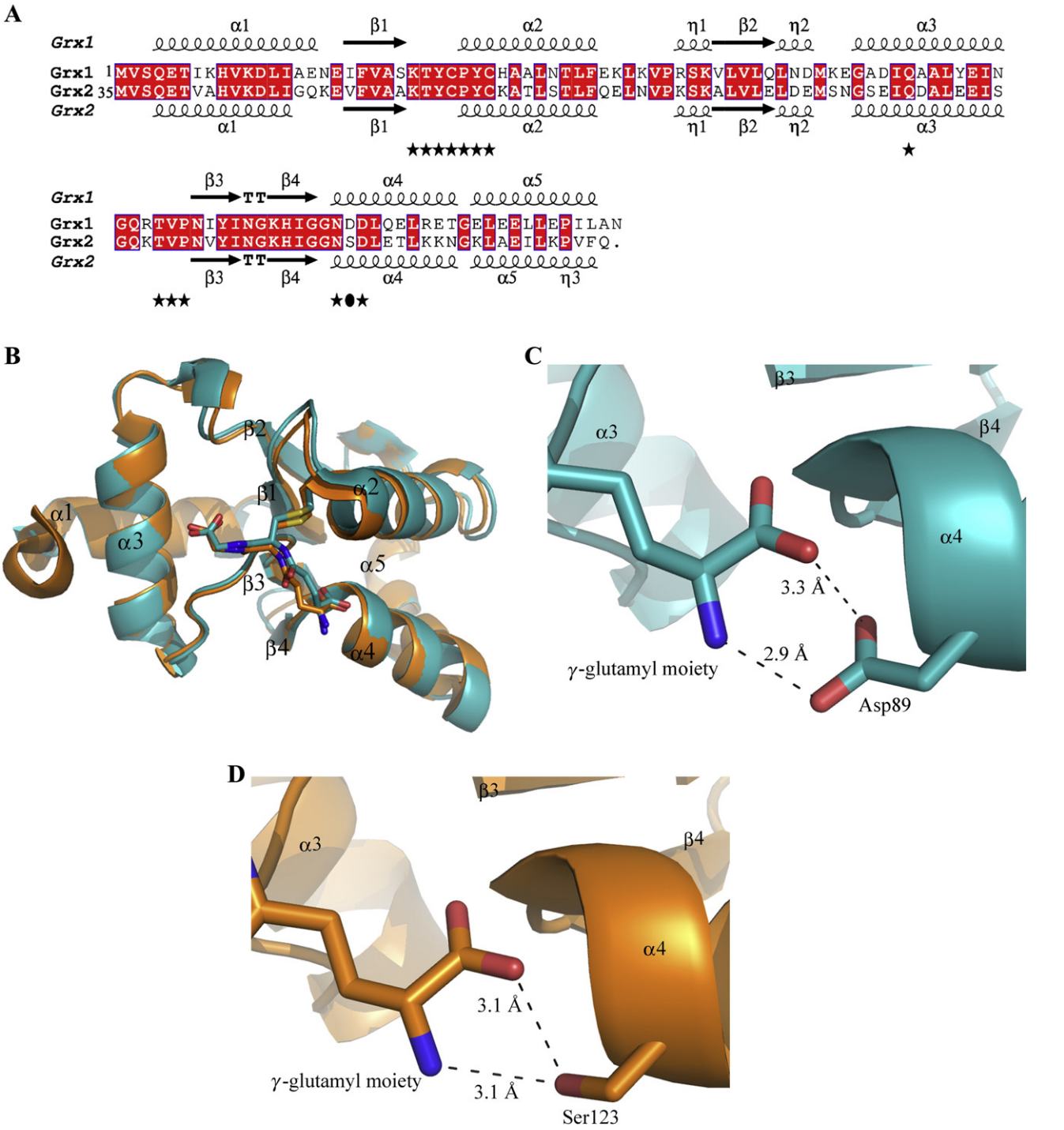

Fig. 2. Comparison of Grx1 and Grx2. A) Sequence alignment of Grx1 and Grx2. The alignment was performed using MultAlin and ESPript (http://prodes.toulouse.inra.fr/multalin) [43,44]. The secondary structural elements are identified with DSSP [45] from structures of oxidized Grx1 (PDB code 3C1R) and oxidized Grx2 (PDB code 3CTF) and displayed at the top and bottom of the alignment, respectively. According to glutathionylated Grx2 [39] and Grx1 [25], residues involved in GSH binding are labeled with stars and filled cycle at the bottom. The divergent GSH binding residue, Asp89 in Grx1 or Ser123 in Grx2, is labeled with a filled cycle. B) Superposition of Grx1 (PDB code: 3C1S, blue) and Grx2 (PDB code: 3D5J, orange), both in the glutathionylated form. A close-up view of the hydrogen bonds between the γ-glutamyl group of GSH and C) Asp89 in Grx1 (PDB code: 3C1S) or D) Ser123 in Grx2 (PDB code: 3D5J).

concentration of 240 nM for Grx1 and 40 nM for Grx2, the apparent K_m and V_{max} values towards β-ME-SG were determined by non-linear regression of Michaelis–Menten plots (Fig. 3A and B). Compared to Grx1, Grx2 possesses a lower affinity (about one fourth) towards β-ME-SG, but a much higher turnover number (about thirteen folds). Thus, Grx2 has a specific activity (k_{cat}/K_m) of approximately three folds to that of Grx1. These kinetic constants of Grx1/Grx2 towards HED/β-ME-SG are in agreement with the results of Discola's [39].

Grx1 and Grx2 share an identity of 64% and similarity of 85%, and moreover, they share an also identical GSH binding site, except for a single residue change from Asp89 in Grx1 to Ser123 in Grx2 (Fig.2A). In order to address whether the different enzymatic activities of Grx1 and Grx2 are due to this different residue, we constructed the mutants Grx1D89S and Grx2S123D to compare their HEDS activities at a fixed GSH concentration of 1 mM (Fig. 3C and D). Grx1D89S presents, compared to the wide-type Grx1, a higher K_m (about three folds) and

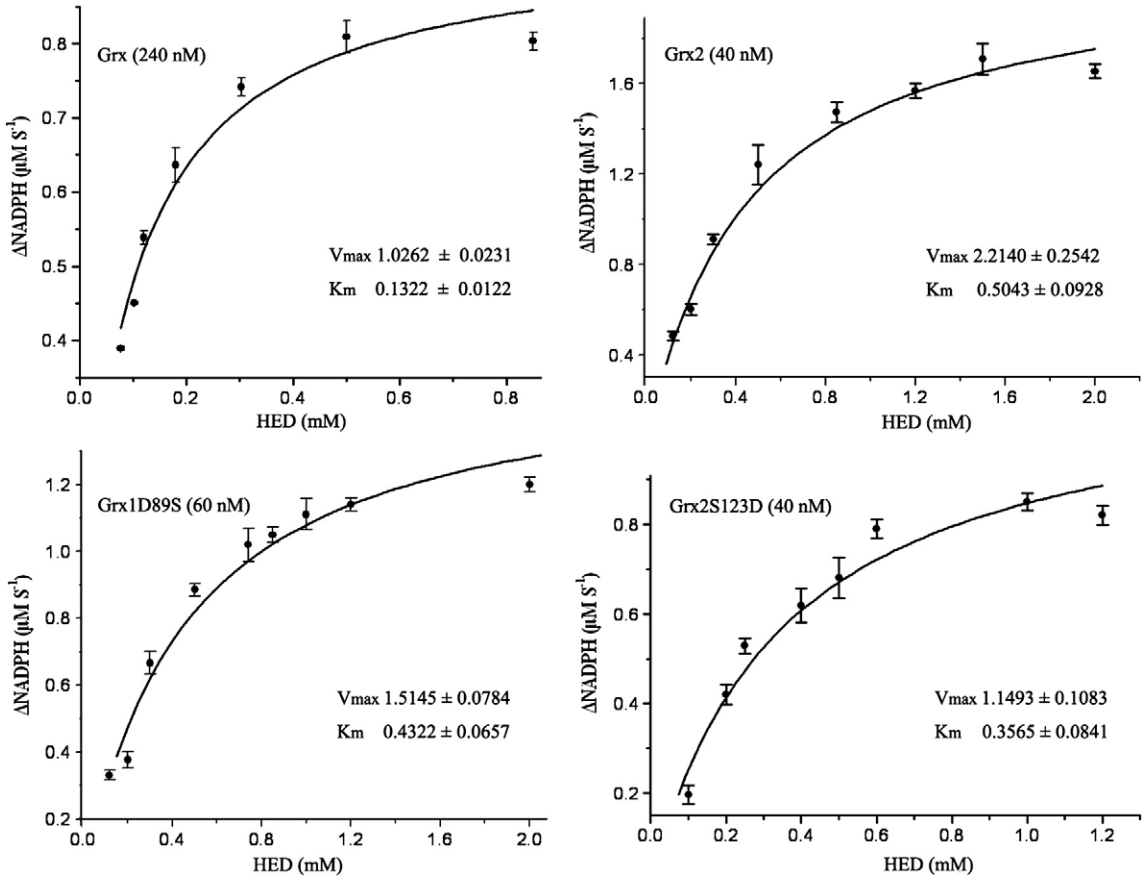

Fig. 3. Activity comparison. HEDS assays of A) Grx1, B) Grx2, C) Grx1D89S and D) Grx2S123D. Plots of velocity against substrate concentration were used for the determination of the kinetic constants. The reaction mixture, containing 100 mM Tris–HCl, pH 7.4, 0.25 mM NADPH, 6 μg/ml yeast glutathione reductase (GR, Sigma-Aldrich), 0.07–2.5 mM HEDS at fixed 1 mM concentration of GSH.

a higher k_{cat} (about six folds) values towards β-ME-SG, leading to a higher specific activity (k_{cat}/K_m value, about two folds). This demonstrated that the mutation of Asp89 to Ser could increase the HEDS activity of Grx1, which is closer to that of Grx2. In contrast, the Grx2S123D has a lower K_m (seven tenth) and a lower k_{cat} (one half) values towards β-ME-SG, compared to that of the wide-type Grx2. Moreover, we also determined the apparent k_{cat} and K_M of Grx1, Grx2 and their mutants towards β-ME-SG at various GSH concentrations, and revealed similar results (Table 2). Either mutation of D89S in Grx1 or S123D in Grx2 will make one assemble the other, from the view points of both substrate binding affinity (as indicated by the K_m values) and enzymatic activity (as shown by the k_{cat} values). Taken together, D89 and S123 play crucial role in the substrate binding and enzymatic activity of Grx1 and Grx2, respectively, and differ these two Grxs from each other.

Phylogenetic analysis demonstrated that Grx1 and Grx2 evolved from a common ancestor [41,42]. But why both copies are functional and what finely differs one from the other? In accordance to their physiological divergence during normal growth and stress conditions, they are under the control of different transcriptional factors (http://db.yeastgenome.org/cgi-bin/gbrowse/scgenome/), and localized in various subcellular compartments. Moreover, there are 31,400 and 3030 molecules of Grx2 and Grx1, respectively, in a yeast cell during normal growth conditions (http://db.yeastgenome.org/). Thus, we concluded the different affinity towards substrate between Grx1 and Grx2 might be evolved in concert with the distinct concentrations or expression levels at their specialized localization.

Acknowledgements

This research was supported by the projects 2006CB910202 and 2006CB806501 from the Ministry of Science and Technology of China, the grant 30870490 from Chinese National Natural Science Foundation.

Table 2
Apparent kinetic constants for the reduction of the mixed disulfide formed between GSH and HED by Grx1, Grx2, Grx1D89S, and Grx2S123D.

GSH (mM)	0.5		1.0		1.5		2.0	
	k_{cat}^{app} (S^{-1})	K_m^{app} (mM)	k_{cat}^{app} (S^{-1})	K_m^{app} (mM)	k_{cat}^{app} (S^{-1})	K_m^{app} (mM)	k_{cat}^{app} (S^{-1})	K_m^{app} (mM)
Grx1	3.7 ± 0.2	0.11 ± 0.02	4.3 ± 0.5	0.13 ± 0.01	4.9 ± 0.3	0.14 ± 0.01	5.2 ± 0.3	0.14 ± 0.03
Grx2	41.4 ± 0.3	0.53 ± 0.03	55.0 ± 3.2	0.50 ± 0.03	55.3 ± 4.1	0.50 ± 0.12	61.0 ± 4.2	NA
Grx1D89S	20.4 ± 0.3	0.45 ± 0.06	25.2 ± 1.4	0.43 ± 0.03	25.8 ± 1.9	0.41 ± 0.08	33.4 ± 2.6	NA
Grx2S123D	15.8 ± 0.2	0.39 ± 0.04	28.5 ± 2.5	0.35 ± 0.02	28.2 ± 2.1	0.33 ± 0.05	33.2 ± 1.9	NA

The reaction mixture consists of 100 mM Tris–HCl, pH 7.4, 6 μg/ml GR and 0.25 mM NADPH. The concentration of HED is varied from 0.074 to 2.5 mM for each fixed concentration of GSH (0.5, 1.0, 1.5 or 2.0 mM), the reaction is triggered by the addition of 240 nM Grx1, 60 nM Grx1D89S, 40 nM Grx2 or 40 nM Grx2S123D, respectively. When the GSH concentration was set to 2 mM or higher, neither of the data from Grx2, Grx1D89S or Grx2S123D fit the Michalis–Menten plots, so the K_m values were not available (NA).

References

[1] B.P. Yu, Cellular defenses against damage from reactive oxygen species, Physiol. Rev. 74 (1994) 139–162.
[2] B. Halliwell, J.M.C. Gutteridge, Free Radicals in Biology and Medicine, 2nd ednOxford University Press, Oxford, 1989.
[3] J.M. Gutteridge, Free radicals in disease processes: a compilation of cause and consequence, Free radic. res. commun. 19 (1993) 141–158.
[4] B. Demple, A bridge to control, Science 279 (1998) 1655–1656.
[5] A. Rietsch, J. Beckwith, The genetics of disulfide bond metabolism, Annu. Rev. Genet. 32 (1998) 163–184.
[6] E.J. Stewart, F. Åslund, J. Beckwith, Disulfide bond formation in the *Escherichia coli* cytoplasm: an *in vivo* role reversal for the thioredoxins, Embo J 17 (1998) 5543–5550.
[7] O. Carmel-Harel, G. Storz, Roles of the glutathione- and thioredoxin-dependent reduction systems in the *Escherichia coli* and *Saccharomyces cerevisiae* responses to oxidative stress, Annu. Rev. Microbiol. 54 (2000) 439–461.
[8] A. Holmgren, Thioredoxin and glutaredoxin systems, J Biol Chem 264 (1989) 13963–13966.
[9] A.P. Fernandes, A. Holmgren, Glutaredoxins: glutathione-dependent redox enzymes with functions far beyond a simple thioredoxin backup system, Antioxid. Redox Signal. 6 (2004) 63–74.
[10] E.J. Collinson, C.M. Grant, Role of yeast glutaredoxins as glutathione S-transferases, J. Biol. Chem. 278 (2003) 22492–22497.
[11] D.W. Starke, P.B. Chock, J.J. Mieyal, Glutathione-thiyl radical scavenging and transferase properties of human glutaredoxin (thioltransferase). Potential role in redox signal transduction, J Biol Chem 278 (2003) 14607–14613.
[12] H. Murata, Y. Ihara, H. Nakamura, J. Yodoi, K. Sumikawa, T. Kondo, Glutaredoxin exerts an antiapoptotic effect by regulating the redox state of Akt, J Biol Chem 278 (2003) 50226–50233.
[13] J.J. Song, J.G. Rhee, M. Suntharalingam, S.A. Walsh, D.R. Spitz, Y.J. Lee, Role of glutaredoxin in metabolic oxidative stress. Glutaredoxin as a sensor of oxidative stress mediated by H2O2, J Biol Chem 277 (2002) 46566–46575.
[14] S.A. Gravina, J.J. Mieyal, Thioltransferase is a specific glutathionyl mixed disulfide oxidoreductase, Biochemistry 32 (1993) 3368–3376.
[15] C.H. Jung, J.A. Thomas, S-glutathiolated hepatocyte proteins and insulin disulfides as substrates for reduction by glutaredoxin, thioredoxin, protein disulfide isomerase, and glutathione, Arch. Biochem. Biophys. 335 (1996) 61–72.
[16] H.F. Gilbert, Molecular and cellular aspects of thiol-disulfide exchange, Adv. Enzymol. Relat. Areas Mol. Biol. 63 (1990) 169–172.
[17] J.A. Thomas, B. Poland, R. Honzatko, Protein sulfhydryls and their role in the antioxidant function of protein S-thiolation, Arch. Biochem. Biophys. 319 (1995) 1–9.
[18] E. Eckers, M. Bien, V. Stroobant, J.M. Herrmann, M. Deponte, Biochemical characterization of dithiol glutaredoxin 8 from *Saccharomyces cerevisiae*: the catalytic redox mechanism redux (dagger), Biochemistry (2009).
[19] S. Luikenhuis, G. Perrone, I.W. Dawes, C.M. Grant, The yeast *Saccharomyces cerevisiae* contains two glutaredoxin genes that are required for protection against reactive oxygen species, Mol. Biol. Cell 9 (1998) 1081–1091.
[20] M.T. Rodriguez-Manzaneque, J. Ros, E. Cabiscol, A. Sorribas, E. Herrero, Grx5 glutaredoxin plays a central role in protection against protein oxidative damage in *Saccharomyces cerevisiae*, Mol. Cell. Biol. 19 (1999) 8180–8190.
[21] A. Izquierdo, C. Casas, U. Muhlenhoff, C.H. Lillig, E. Herrero, *Saccharomyces cerevisiae* Grx6 and Grx7 are monothiol glutaredoxins associated with the early secretory pathway, Eukaryot Cell 7 (2008) 1415–1426.
[22] M.T. Rodriguez-Manzaneque, J. Tamarit, G. Belli, J. Ros, E. Herrero, Grx5 is a mitochondrial glutaredoxin required for the activity of iron/sulfur enzymes, Mol. Biol. Cell 13 (2002) 1109–1121.
[23] L. Ojeda, G. Keller, U. Muhlenhoff, J.C. Rutherford, R. Lill, D.R. Winge, Role of glutaredoxin-3 and glutaredoxin-4 in the iron regulation of the Aft1 transcriptional activator in *Saccharomyces cerevisiae*, J Biol Chem 281 (2006) 17661–17669.
[24] R. Lill, U. Muhlenhoff, Iron–sulfur protein biogenesis in eukaryotes: components and mechanisms, Annu. Rev. Cell Dev. Biol. 22 (2006) 457–486.
[25] J. Yu, N.N. Zhang, P.D. Yin, P.X. Cui, C.Z. Zhou, Glutathionylation-triggered conformational changes of glutaredoxin Grx1 from the yeast *Saccharomyces cerevisiae*, Proteins-Struct. Funct. Bioinform. 72 (2008) 1077–1083.
[26] J.R. Pedrajas, P. Porras, E. Martinez-Galisteo, C.A. Padilla, A. Miranda-Vizuete, J.A. Barcena, Two isoforms of *Saccharomyces cerevisiae* glutaredoxin 2 are expressed in vivo and localize to different subcellular compartments, Biochem. J. 364 (2002) 617–623.
[27] P. Porras, C.A. Padilla, M. Krayl, W. Voos, J.A. Barcena, One single in-frame AUG codon is responsible for a diversity of subcellular localizations of glutaredoxin 2 in *Saccharomyces cerevisiae*, J Biol Chem 281 (2006) 16551–16562.
[28] K. Bartels, C. Klein, AUTOMAR User's Guide, v.1.4. Nov. 11, 2003, http://www.marresearch.com/automar2003Available at.
[29] A.T. Brunger, P.D. Adams, G.M. Clore, W.L. DeLano, P. Gros, R.W. Grosse-Kunstleve, J.S. Jiang, J. Kuszewski, M. Nilges, N.S. Pannu, R.J. Read, L.M. Rice, T. Simonson, G.L. Warren, Crystallography & NMR system: a new software suite for macromolecular structure determination, Acta Crystallogr D 54 (1998) 905–921.
[30] T.A. Jones, J.Y. Zou, S.W. Cowan, Kjeldgaard, Improved methods for building protein models in electron density maps and the location of errors in these models, Acta Crystallogr. A 47 (Pt 2) (1991) 110–119.
[31] G.N. Murshudov, A.A. Vagin, E.J. Dodson, Refinement of macromolecular structures by the maximum-likelihood method, Acta Crystallogr D 53 (1997) 240–255.
[32] R.A. Laskowski, M.W. MacArthur, D.S. Moss, J.M. Thornton, PROCHECK: a program to check the stereochemical quality of protein structures, J Appl Crystallogr 26 (1993) 283–291.
[33] W.L. DeLano, The PyMOL Molecular Graphics System, http://www.pymol.org2002.
[34] A. Holmgren, F. Aslund, Glutaredoxin, Methods Enzymol. 252 (1995) 283–292.
[35] J.P. Bacik, B. Hazes, Crystal structures of a poxviral glutaredoxin in the oxidized and reduced states show redox-correlated structural changes, J Mol Biol 365 (2007) 1545–1558.
[36] N. Foloppe, L. Nilsson, Stabilization of the catalytic thiolate in a mammalian glutaredoxin: structure, dynamics and electrostatics of reduced pig glutaredoxin and its mutants, J Mol Biol 372 (2007) 798–816.
[37] E. Moutevelis, J. Warwicker, Prediction of pKa and redox properties in the thioredoxin superfamily, Protein Sci. 13 (2004) 2744–2752.
[38] Y.F. Yang, W.W. Wells, Identification and characterization of the functional amino acids at the active center of pig liver thioltransferase by site-directed mutagenesis, J Biol Chem 266 (1991) 12759–12765.
[39] K.F. Discola, M.A. de Oliveira, J.R. Rosa Cussiol, G. Monteiro, J.A. Barcena, P. Porras, C.A. Padilla, B.G. Guimaraes, L.E. Netto, Structural aspects of the distinct biochemical properties of glutaredoxin 1 and glutaredoxin 2 from Saccharomyces cerevisiae, J Mol Biol 385 (2009) 889–901.
[40] C.H. Lillig, C. Berndt, A. Holmgren, Glutaredoxin systems, Biochim. Biophys. Acta 1780 (2008) 1304–1317.
[41] J. Sagemark, T.H. Elgan, T.R. Burglin, C. Johansson, A. Holmgren, K.D. Berndt, Redox properties and evolution of human glutaredoxins, Proteins 68 (2007) 879–892.
[42] N. Mesecke, A. Spang, M. Deponte, J.M. Herrmann, A novel group of glutaredoxins in the cis-Golgi critical for oxidative stress resistance, Mol. Biol. Cell 19 (2008) 2673–2680.
[43] F. Corpet, Multiple sequence alignment with hierarchical clustering, Nucleic Acids Res. 16 (1988) 10881–10890.
[44] P. Gouet, X. Robert, E. Courcelle, ESPript/ENDscript: extracting and rendering sequence and 3D information from atomic structures of proteins, Nucleic Acids Res. 31 (2003) 3320–3323.
[45] W. Kabsch, C. Sander, Dictionary of protein secondary structure: pattern recognition of hydrogen-bonded and geometrical features, Biopolymers 22 (1983) 2577–2637.